Optical, electrical and mechanical properties of TiN thin film obtained from a TiO2 sol-gel coating and rapid thermal nitridation

Arnaud Valour, Maria Alejandra Usuga-Higuita, Gaylord Guillonneau, Nicolas Crespo-Monteiro, Damien Jamon, Marion Hochedel, Jean-Yves Michalon, Stéphanie Reynaud, Francis Vocanson, Carmen Jiménez, et al.

Surface & Coatings Technology 413 (2021) 127089

Contents lists available at ScienceDirect

Surface & Coatings Technology

journal homepage: www.elsevier.com/locate/surfcoat

Optical, electrical and mechanical properties of TiN thin film obtained from a TiO_2 sol-gel coating and rapid thermal nitridation

Arnaud Valour [a], Maria Alejandra Usuga Higuita [a], Gaylord Guillonneau [b], Nicolas Crespo-Monteiro [a,*], Damien Jamon [a], Marion Hochedel [a], Jean-Yves Michalon [a], Stéphanie Reynaud [a], Francis Vocanson [a], Carmen Jiménez [c], Michel Langlet [c], Christophe Donnet [a], Yves Jourlin [a,*]

[a] Université de Lyon, Laboratoire Hubert Curien, UMR CNRS 5516, 42000 Saint-Etienne, France
[b] Ecole Centrale de Lyon, Laboratoire de Tribologie et Dynamique des Systèmes UMR 5516, 69131 Ecully, France
[c] Université de Grenoble Alpes, Laboratoire des Matériaux et du Génie Physique, UMR CNRS 5628, 38000 Grenoble, France

ARTICLE INFO

Keywords:
Titanium nitride
Sol-gel method
Rapid thermal nitridation
Mechanical
Electrical
Optical properties

ABSTRACT

This study reports the optical, electrical and mechanical properties of TiN films prepared by direct rapid thermal nitridation process from a photo-patternable TiO_2 sol-gel layer. The sol-gel approach is compatible to non-planar and large substrates and allows the micro-nanotexturing of crystallized TiN surfaces in a significantly short time, large scale and at a lower cost compared to TiN layer deposition from existing and conventional processes (CVD, PVD, ALD…). In this paper, the optical measurements are carried out by optical spectroscopy in the UV, visible and near-IR region and by ellipsometry. The resistivity and the conductivity are estimated by four-point probe method, while hardness is characterized by nano-indentation experiments. The results indicate that the TiN thin film made by sol-gel method and rapid thermal nitridation are very promising for the manufacturing of optical metasurfaces devices or new plasmonic materials.

1. Introduction

Metal-nitrides are very promising in the plasmonic materials field or metasurface devices. Among them, titanium nitride (TiN) is one of the most investigated compounds to date [1–3]. Indeed, TiN has intrinsic physico-chemical and optical properties making it first-choice material: low resistivity, high reflectance in the infrared spectral range, good corrosion resistance, good chemical inertness, good thermal stability, and high hardness [4–6]. Generally, TiN thin layer is obtained using a wide range of deposition processes requiring vacuum technology, such as reactive magneton sputtering [1,7–10], molecular-beam epitaxy [11,12], chemical vapor deposition (CVD) [13–15], atomic layer deposition (ALD) [16–19] or pulsed laser deposition (PLD) [20–22], under a nitrogen or ammonia atmosphere. Unfortunately, due to its good hardness and chemical resistance, TiN is not adapted for being micro or nanostructured using standard etching process (Reactive Ion Etching for example). To overcome this technological lock, the structuring of TiN by sol-gel process seems promising because of its simplicity of implementation, its low cost and its compatibility to unconventional substrates (non-planar and curve substrates). In a previous work, we have shown that this method can be implemented by performing micro-nano structuring on a photopatternable TiO_2 sol-gel film, deposited from a photosensitive sol, that is then converted into micro-nanostructured TiO_xN_y using a high temperature thermal nitridation process in an ammoniac atmosphere [23]. More recently, we have presented an innovative and direct rapid thermal nitridation (RTN) process allowing us to obtain micro-nanotextured crystallized TiN surfaces in significantly less stringent conditions [24]. RTN appears to be a very promising alternative way to synthetize high-quality submicro-structured TiN thin films with complex shapes on a wide range of substrates. In this paper, we focus on optical, electrical and mechanical properties of TiN thin film obtained by direct RTN process from a photo-patternable TiO_2 sol-gel layer. To our knowledge, the study of these properties, for a TiN thin layer obtained by RTN process, has never been yet demonstrated. Therefore, these first characterizations were performed on non-photo-patterned thin films. The optical measurements are carried out by optical spectroscopy in the UV, visible and near-IR region and by ellipsometry. The resistivity and the conductivity are estimated by four-point

* Corresponding authors.
E-mail addresses: nicolas.crespo.monteiro@univ-st-etienne.fr (N. Crespo-Monteiro), yves.jourlin@univ-st-etienne.fr (Y. Jourlin).

https://doi.org/10.1016/j.surfcoat.2021.127089
Received 16 October 2020; Received in revised form 4 March 2021; Accepted 13 March 2021
Available online 19 March 2021

probe method, and hardness is studied by nano-indentation experiments. Values of these properties are compared to TiN films obtained by conventional layer deposition processes (PVD, CVD, ALD).

2. Materials and methods

2.1. Elaboration of TiO_2 sol-gel layer

Using a specific sol-gel technique previously published and detailed in the references [23,25–27], TiO_2 thin film was elaborated from a mixture of two sols at room temperature. In summary, the first sol was elaborated by mixing tetraisopropylorthotitanate (TIPT from Aldrich) with deionized water, hydrochloric acid (HCl from Roth), and butyl alcohol (BuOH from Alfa Aesar) as a solvent. The TIPT concentration in the solution was 0.4 M, and the TIPT/H_2O/HCl/BuOH molar composition was 1/0.82/0.13/23.9. The second sol was prepared from TIPT complexed by benzoylacetone (BzAc from Aldrich) in methyl alcohol (MeOH from Sigma-Aldrich). The TIPT/BzAc/MeOH molar composition was 1/0.91/20.4. The photosensitive TiO_2 sol-gel was obtained by mixing the two sols in order to form a final sol with a TIPT concentration of 0.6 M and a BzAc/TIPT molar ratio of 0.6. The TiO_2 sol was coated on a silicate substrate (for electrical and optical characterizations) or on silicon substrate (for mechanical measurements) by using spin coating technique at the speed of 3000 rpm during 30 s. The obtained sol-gel film was heated at 110 °C during 90 min, leading to a so-called xerogel film (for convenience, we will keep in the rest of the manuscript the name TiO_2 for a xerogel comprising organic functions), with a thickness close to 300 nm on silica substrate and 280 nm on silicon substrate.

2.2. Rapid thermal nitridation of TiO_2 thin film

Rapid thermal nitridation treatment of the TiO_2 film was performed in a reproducible and uniform process using pure NH_3 gas under a halogen infrared lamp-heated furnace (RTA As-One 100 from Annealsys). Initially, the reactor was purged with a cycle of N_2 (1000 sccm) and vacuum. The samples are then irradiated for 30 s at 30% of the lamp power 10 times, with 1 s at 1% of the lamp power between each heat treatment to preserve the lamp and maximize its lifetime. Thus, the thermal exposure process with the 10 cycles lasted 10 min. During the nitridation process, a 1000 sccm NH_3 flow was introduced in the chamber at a pressure of 10 mbar.

2.3. Structural and optical measurements

The films were characterized before and after nitriding process. Spectrophotometric measurements (Cary 5000 UV–Vis-NIR from Agilent Technologies) were performed in the infrared, visible and near-UV region. Reflection spectroscopy measurement was carried out in specular configuration with an incident angle of 10°. Spectroscopic ellipsometry measurements (UVISEL from Horiba Jobin Yvon, associated with DeltaPsi2 software) were carried out in order to determine the thickness, the refractive index (n) and the extinction coefficient (k) leading then to the corresponding ε' and ε'' values of permittivity of the TiO_2 and TiN thin films. Ellipsometry measurements were performed with an angle of incidence of 60°, in the 0.7 to 4.5 eV spectral range with a 0.02 eV step. The optical model consists in 2 layers on a semi-infinite glass substrate. The first layer is made of the material under consideration. The second layer is considered as a roughness layer, with a 50%–50% mixed dielectric function between void and the dielectric function of the first layer. For the TiO_2 material, we used a double Tauc Lorentz dispersion formula. For TiN material, we used the classical dispersion model, based on the sum of the single and double Lorentz, and Drude oscillators [28]. Phase composition of the layer after the RTN process was analyzed using Raman micro spectroscopy measurements (LabRam ARAMIS) with excitation at 633 nm (He—Ne laser). Investigation of the roughness of the surface of the films was performed by interferometric confocal microscopy (Contour GT-K1, Bruker) with a white light source, allowing to obtain roughness mappings of the film surfaces, as well as their arithmetic (Ra) and quadratic (Rq) roughness coefficients.

2.4. Electrical measurements

Resistivity measurements were performed by the four-point probe method. The surface resistance has been measured in ten different places of TiO2 and TiN layers deposited on rectangular silica substrates of 20 mm wide × 15 mm length. The mean resistivity value was then derived according to the samples thickness that was measured with a profilometer Veeco Dektak 3 ST.

2.5. Transmission electron microscopy characterization

Structural investigations were conducted with electron microscopy. Firstly, focused ion beam (FIB) lamellas were extracted from the two samples using a FEI (Thermofisher) Helios 600i dual beam FIB/SEM microscope. The two lamellas were thinned at different Ga^+ ion voltages and currents, and were finally thoroughly cleaned down to 1 kV in order to optimally remove ion beam artifacts, such as re-deposition or amorphization. Then, high-angle annular dark field scanning transmission electron microscopy (HAADF STEM) was performed on the lamellas with a JEOL Neo-ARM 200F Transmission Electron Microscope.

2.6. Mechanical characterization

The hardness of the TiO_2 film precursor and TiN film was determined from load-displacement curves obtained with a commercial MTS Nanoindenter XP apparatus carried out in dynamic mode (frequency = 32 Hz, amplitude = 2 nm) with a Berkovich diamond tip. The load, up to 50 mN, was also applied exponentially versus time, in order to keep a constant strain rate $\frac{\dot{P}}{P} = 3.10^{-2}\ s^{-1}$ throughout the loading procedure. Each sample was characterized at ten different locations, in order to check the reproducibility of the measurements. Nano-indentation investigations were first performed on a thick silicon substrate, on which the TiO_2 and TiN films were further tested.

3. Results and discussion

3.1. Structure and surface morphology

After nitration of TiO_2 sol-gel by RTN treatment, the thin film obtained, shown in Fig. 1, clearly indicates the formation of a TiN layer with the Raman bands from the TiN crystalline phase, in accordance

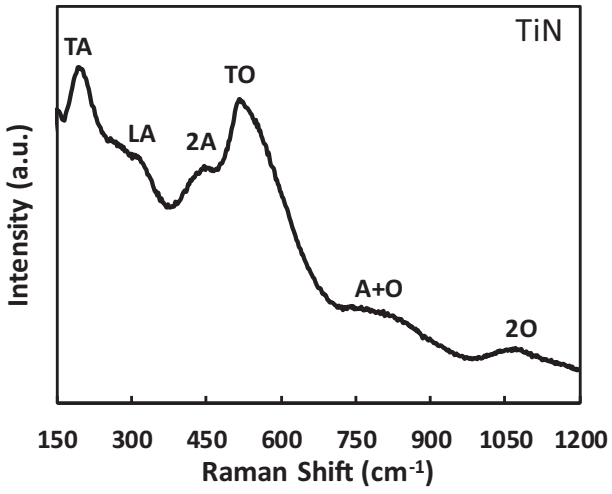

Fig. 1. Raman spectrum of TiN thin film deposited on SiO_2 substrate.

with results reported in previous works [24]. The 210, 318, 447 and 526 cm^{-1} bands observed in the spectrum relate to transverse acoustic (TA), longitudinal acoustic (LA), second-order acoustic (2A) and transverse optical (TO) modes respectively. The two broad bands around 825 and 1085 cm^{-1} are assigned to LA + TO and 2TO modes of TiN.

The quantification of roughness of the initial sol-gel TiO_2 film and its evolution after the conversion into TiN by the thermal nitridation process, is paramount for the characterization of the films and further film properties detailed hereafter. Roughness mapping, over about 130 μm × 100 μm, of the surface of TiO_2 and TiN films deposited on the silicon substrate, are respectively shown on Fig. 2a and d. Arithmetic (Ra) and quadratic (Rq) roughness coefficients, deduced from these mappings, are Ra = 4,9 nm and Rq = 6,1 nm for the TiO_2 surface, and Ra = 3,1 nm and Rq = 3,9 nm for the TiN film. Typical X and Y profiles extracted from the mappings are depicted on Fig. 2b and c for TiO_2, and Fig. 2e and f for TiN. Both film surfaces are rather smooth, in particular the TiN surface consecutive to the nitridation process which does not modify significantly the roughness of the TiO_2 sol gel film.

As shown from high-angle annular dark field scanning transmission electron microscopy (HAADF STEM) images in Fig. 3, the TiN layer is quite porous and thin, with a homogenous thickness around 40–50 nm.

3.2. Optical properties

The UV–Visible-NIR reflectance and transmittance spectra of the slightly yellowish TiO_2 thin layer obtained by spin-coating on silica substrate (shown in Fig. 4a) present a typical strong absorption band of TiO_2 under 400 nm, indicating its absorption in the UV wavelength range. The transmittance spectrum presents no other absorption band in the visible and near infrared range with a maximal transmittance higher than 80%, indicating a good transparency in these regions. The reflectance spectrum agrees with these results, with a reflectance lower than 20% and a slight purple color in reflection. After nitridation, changes in optical properties can be observed as shown in Fig. 4b. We obtained a gold/burnished color, characteristic of pure TiN sample. This is slightly transparent due to the thin thickness (40 nm). The transmittance spectrum of the TiN thin film presents a maximum of 35% at wavelengths around 500 nm and decreases under 5% in the near-infrared region. The reflectance spectrum indicates a minimum of 21% at 500 nm and a high reflection around 70% in near-infrared wavelengths highlighting the metallic character of TiN [29].

The optical constant measured by spectroscopic ellipsometry for the TiO_2 thin films before and after nitridation is presented in Fig. 5.

For TiO_2, the refractive index (n) is calculated around n = 2 and n = 1,7 in the visible (for λ = 400 nm) and near infrared region (for λ from 1100 to 2000 nm), respectively. After nitridation, the thickness of the TiN film is estimated around 40 nm, in accordance with the values determined by profilometry. The refractive index increases close to n = 5 for λ = 2000 nm. The real part of the refractive index differs slightly from the bulk value of the TiN reported in the literature [30]. It can be explained, as previously demonstrated, by some porosity in the layer that slightly reduces this real part.

The k value of the refractive index demonstrates absorption of the TiN thin layer in the infrared range (k = 7 for λ = 2000 nm), while it is close to zero for the TiO_2 thin layer in the visible and infrared ranges. From ellipsometry measurements, we can also deduce the corresponding values of the real (ε′) and the imaginary (ε″) parts of permittivity with the following equations:

$$\varepsilon' = n^2 - k^2, \tag{1}$$

$$\varepsilon'' = 2\,n\,k \tag{2}$$

These parameters allow us to conclude about the metallic properties of the TiN layer. The ε′ and ε″ values are illustrated as a function of the wavelength in Fig. 5 and d, respectively. The film presents the lowest real permittivity around $\varepsilon' \approx -30$ for λ = 2000 nm. Generally, the metallic property is estimated with the absolute value of the real part of the permittivity (ε′) and must be as high as possible to consider a good metal (for example ε′ (Au) < −200 for λ = 2000 nm). Concerning the imaginary part of the permittivity, ε″ evolves almost linearly as a function of the wavelength up to ε″ = 70 in the range of 500 and 2000 nm, which confirms the metallic behavior of the TiN film. It should be

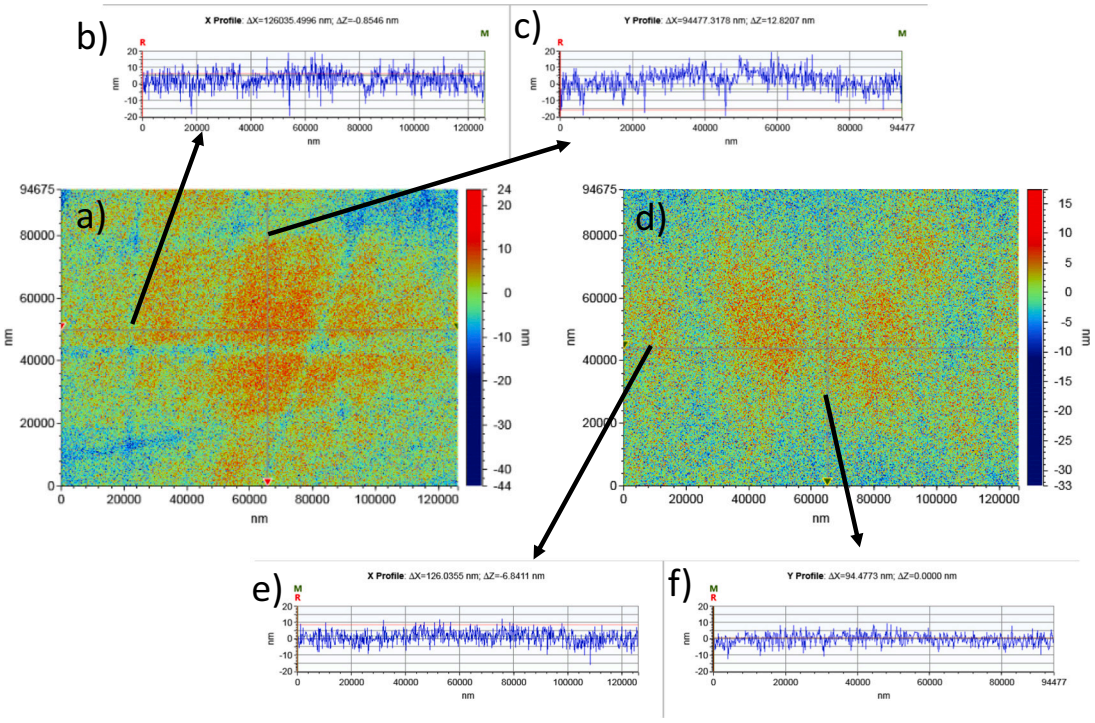

Fig. 2. Roughness mapping of (a) TiO_2 film and (d) TiN film, obtained by interferometric confocal microscopy; (b–c) extracted X and Y profiles for the TiO_2 film; (e–f) extracted X and Y profiles for the TiN film.

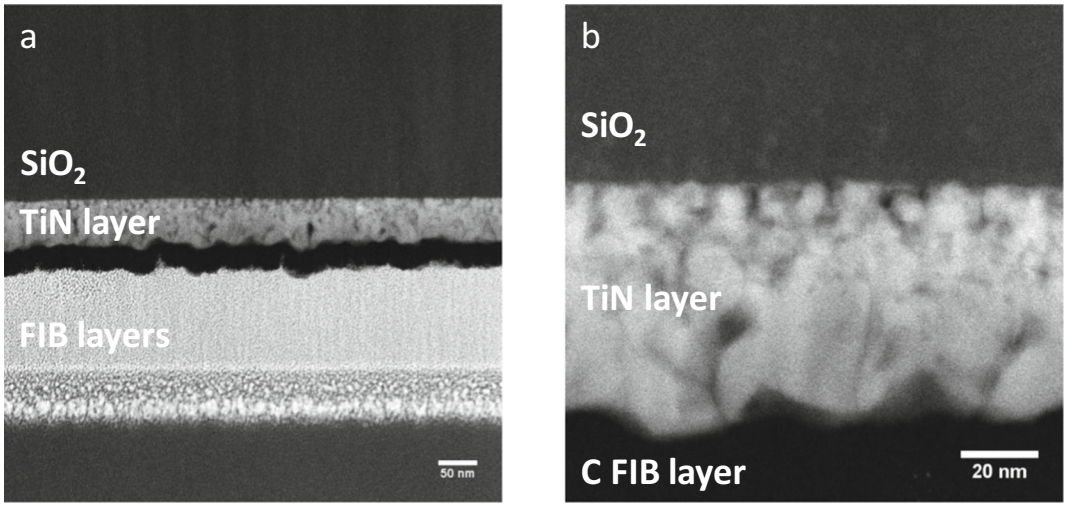

Fig. 3. (a) Cross-sectional HAADF STEM and (b) high-magnification images of the TiN thin film.

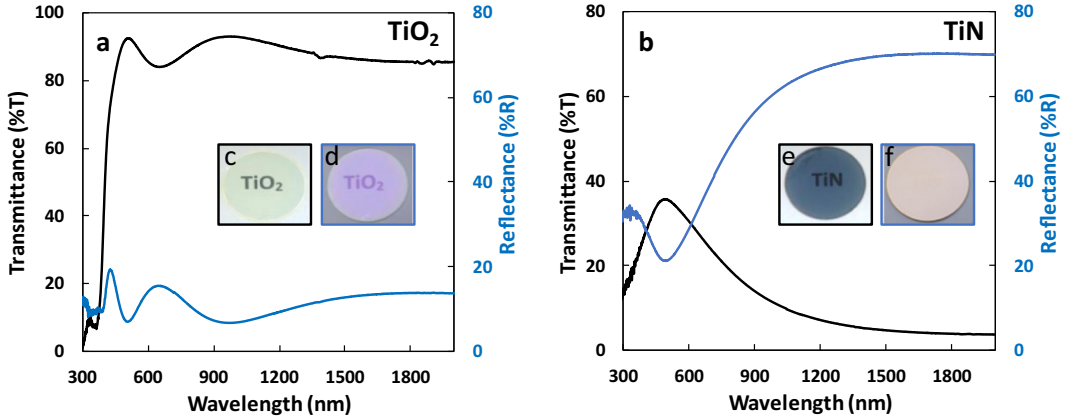

Fig. 4. UV–Visible-NIR reflectance and transmittance spectra of (a) TiO_2 and (b) TiN thin film. Inset (c) and (d): optical photographs of TiO_2 thin films in transmission and specular reflection, respectively. Inset (e) and (f): optical photographs of TiN thin films in transmission and specular reflection, respectively.

noted that these optical results for TiN are also quite similar to those obtained in previous work [24] while the NH_3 flux used during the nitridation process has been divided by two. To conclude from these ellipsometry results, we observe a lower metallic behavior in our TiN film compared to recent reports of plasmonic TiN [21,31], which can be attributed, as discussed above, to the residual porosity due to the preparation method, and thus explains the lower conductivity of the metallic TiN films as discussed previously. However, as mentioned in our previous work [24], these results show that the TiN layer, obtained using a particularly simplified and low cost method, could be potentially used as a plasmonic layer in the NIR range, with reasonably losses. These has been demonstrated by the reflection spectrum of the TM polarized incident beam with a dip in the reflection curve attributed to the excitation of a Surface Plasmon mode, propagating along the metallic layer.

3.3. Electrical properties

The resistivity (ρ) and conductivity (σ) of the layers can be respectively deduced from the Eqs. (3) and (4) with Rs the surface resistance and d the thickness of the layer:

$$\rho = Rs^{*}d, \tag{3}$$

$$\sigma = 1/\rho \tag{4}$$

These measurements are listed in Table 1. On the one hand, the values indicate that the TiO_2 film presents dielectric properties with a high resistivity close to 10^5 μΩ·cm, i.e. a low conductivity around 10^{-5} S/m. The resistivity is greater than that commonly reported for pure TiO_2 because in our case the TiO_2 film actually consists of a xerogel.

On the other hand, the TiN layer has a much higher conductivity of 6.6×10^3 S/cm, i.e. a much lower resistivity of 1.5×10^{-4} μΩ·cm. These features illustrate the metallic character of the TiN layer and confirm the high degree of nitriding obtained during the RTN process of TiO_2. However, this conductivity is about one order of magnitude lower than those found in the literature for pure TiN obtained by physical deposition process (resistivity ~10^{-5} Ω·cm) [33–35]. This difference in resistivity could be attributed to this residual porosity due to the preparation method, since the films prepared by the sol-gel route are generally less dense than those obtained by physical route deposition.

3.4. Mechanical properties

Table 2 depicts the hardness of TiO_2 and TiN films deduced from nano-indentation investigations.

The hardness of the silicon substrate is H = 11 ± 0.5 GPa, in agreement with typical values compiled in [36]. The hardness of the TiO_2 film precursor is quite constant on the first 250 nm of plastic penetration depth of the indentation tip, which is consistent with the TiO_2 film thickness (280 nm). An average hardness value of 0.55 ± 0.05 GPa is deduced from the 10 indentations at a depth rising between 140

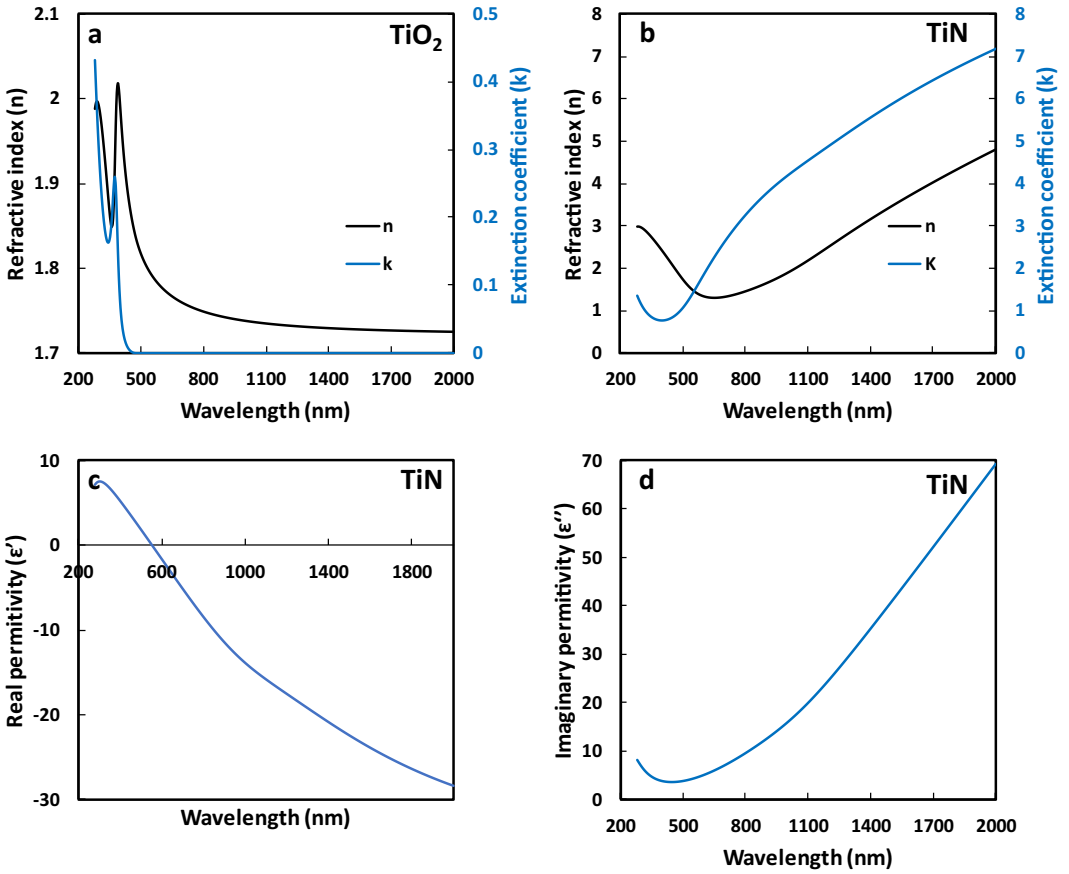

Fig. 5. Refractive index (n) and extinction coefficient (k) according to the wavelength (Vis-NIR) for (a) TiO_2 thin film and (b) TiN. Permittivity according to the wavelength for TiN film: (c) real part (ε′) and (d) imaginary part (ε″).

Table 1
Resistivity and conductivity of the films before (TiO_2) and after (TiN) rapid thermal nitridation treatment.

	ρ (Ω·cm)	σ (S/cm)	Thickness (nm)
TiO_2	8.45×10^4	1.18×10^{-5}	280
TiO_2 literature [32]	2.3×10^4 to 1.0×10^3	/	/
TiN	1.51×10^{-4}	6.64×10^3	40
TiN literature [33]	2.8×10^{-5} to 1.6×10^{-4}	/	/

Table 2
Hardness of the Si substrate, TiO_2 and TiN films deduced from nano-indentation investigations.

Material	Si substrate	TiO_2 film	TiN film
Hardness (GPa)	11.0 ± 0.5	0.55 ± 0.05	10.5 ± 0.5

and 160 nm, which corresponds to the half of the film thickness. This hardness value can thus be considered as representative of the hardness of the sol-gel precursor TiO_2 film. At higher penetration depth, the hardness significantly increases, which is consistent considering the hardness of the silicon substrate. The hardness of the TiN film obtained after conversion of the TiO_2 film precursor by the thermal nitridation process in an ammoniac atmosphere, was estimated to be 10.5 ± 0.5 GPa. This value was obtained by applying the methodology published by Zhou et al. suitable on the commercial nano-indentor, to extract the mechanical properties of a very thin film deposited on a substrate, and available on the MTS Nanoindenter XP used for our samples [37]. More especially, the hardness was not calculated here using classical method since the contact area calculated using the classical contact models (Oliver and Pharr model, Loubet et al. model [38,39]) leads to errors for penetration depths close to the film thickness (the hardness calculation was performed at depths between 30 and 50 nm) [40]. The hardness calculation using the Zhou et al. method requires also that the material modulus is known and homogeneous at the depth range where the hardness is calculated [40]. We assume, for the depths range used to calculate the hardness, the reduced contact modulus is equal to the indenter/substrate modulus (150 GPa). We assume here, the film elasticity is negligible comparing the tip/substrate elasticity. This is an important hypothesis, but seems realistic because the film is very thin, and the penetration depths where the hardness is calculated is very close to the substrate [40]. Such a hardness value appears to be in the lowest range of usual TiN films, which exhibit hardness values within 10–25 GPa depending on their microstructure [41]. As discussed above for resistivity, hardness values of films prepared by sol-gel methods are generally lower compared to other synthesis methods, in agreement with a less dense and more porous microstructure. Let's pay attention the hardness value of TiN film must be considered with care, since the film is very thin and the hardness measurement of very thin layers is extremely complex to determine by nanoindentation at this range of depths, even using the Zhou et al. method. More especially, the tip defect, even very small, can have an influence on the plastic zone around the tip and the contact pressure at low depths, affecting the hardness value. The objective is not to extract the exact hardness value of the TiN film but more an order of magnitude, which seems to be in the range of literature values. This order of magnitude would be helpful, in future studies related to TiN synthesis from sol-gel process, to go further in the quantification of the mechanical properties of TiN films obtained in similar conditions.

4. Conclusions

This study investigates the first attempt to synthetize TiN thin film prepared from TiO_2 sol-gel layer by the rapid thermal nitridation process, by investigating their optical, electrical and mechanical properties. The nitridation condition results in a TiN layer with a maximal recorded optical reflectance about 70% in the near-IR region, a refractive index n = 5 and an extinction coefficient k = 7 for λ = 2000 nm. Ellipsometry measurements also indicated a metallic character in our TiN film close to the literature. The metallicity was also highlighted by electrical measurements with a conductivity of 6.6×10^3 S/cm and a resistivity of 1.5×10^{-4} μΩ·cm while the hardness of the as-deposited TiN thin film was about 10.5 GPa. The authors explain these differences from the existing and residual porosity of the initial TiO_2 sol-gel layer. From this study, we have shown that this TiN layer has interesting properties, even if metallic characteristics and hardness value are rather in the lower range of usual TiN films obtained from conventional layer deposition techniques. The residual porosity, inherent to the sol-gel route, comes from the existing and residual porosity of the TiO_2 sol-gel coupled with the low thickness of the resulting TiN layer, and it could explain these low values. In future works, we will be focused on the optimization of the TiO_2 preparation and/or the nitriding conditions of the TiO_2 thin film in order to increase the thickness of the films and vary the porosity/rugosity to verify these hypotheses. Such optical, electrical and mechanical properties of TiN thin films are very promising because the sol-gel route is the unique technological route enabling the microstructuring of TiN thin layer on non-planar and large substrates, based on dip, spin or spray coating of direct photopatternable TiO_2 based sol-gel.

Funding

The authors would like to thank the French Region Auvergne-Rhône-Alpes for its financial support, in the framework of Pack Ambition Recherche 2018 (MICROSOLEN project) as well as IDEX Lyon (University of Lyon) within the Scientific Breakthrough program (IPPON Project). This work was partly supported by the French RENATECH+ network led by the CNRS, on the NanoSaintEtienne platform.

CRediT authorship contribution statement

A.V., N.C.-M., C.D and Y.J. conducted the study; M.A.U.H and M.H synthesized and deposited the films with supervision from F.V.; A.V. and J.-Y.M. performed the nitridation of the films. The different characterizations were performed as follows: A.V, M-H and N.C.-M. performed optical spectroscopy, S.R. performed STEM-HAADF. D.J. realized ellipsometry measurement, M.A.U.H realized the electrical measurement with help of C.J. and M.L. G.G. provided expertise on the nano-indentation investigations. Y.J. offered suggestions and commented on data analyses. The paper was written by A.V., N.C.-M. and C.D with contributions from G.G., M.L and Y.J.

Declaration of competing interest

The authors declare that they have no known competing financial interests or personal relationships that could have appeared to influence the work reported in this paper.

Acknowledgments

The authors would like to thank Jean-Luc Loubet and Sophie Pavan for nano-indentation experiments and discussion on mechanical investigations.

References

[1] G.V. Naik, J.L. Schroeder, X. Ni, A.V. Kildishev, T.D. Sands, A. Boltasseva, Titanium nitride as a plasmonic material for visible and near-infrared wavelengths, Opt. Mater. Express, OME. 2 (2012) 478–489.
[2] W. Li, U. Guler, N. Kinsey, G.V. Naik, A. Boltasseva, J. Guan, V.M. Shalaev, A. V. Kildishev, Refractory plasmonics with titanium nitride: broadband metamaterial absorber, Adv. Mat. 26 (2014) 7959–7965.
[3] S.M. Choudhury, D. Wang, K. Chaudhuri, C. DeVault, A.V. Kildishev, A. Boltasseva, M. Shalaev, Material platforms for optical metasurfaces, Nanophotonics. 7 (2018) 959–987.
[4] G. Gagnon, J.F. Currie, G. Bêïque, J.L. Brebner, S.C. Gujrathi, L. Ouellet, Characterization of reactively evaporated TiN layers for diffusion barrier applications, J. App. Phys. 75 (1994) 1565–1570.
[5] R.A. Andrievski, Z.M. Dashevsky, G.V. Kalinnikov, Conductivity and the Hall coefficient of nanostructured titanium nitride films, Tech. Phys. Lett. 30 (2004) 930–932.
[6] M.S.R.N. Kiran, M.G. Krishna, K.A. Padmanabhan, Growth, surface morphology, optical properties and electrical resistivity of ε-TiNx ($0.4 < x \leq 0.5$) films, App. Surf. Sci. 255 (2008) 1934–1941.
[7] T.-S. Kim, S.-S. Park, B.-T. Lee, Characterization of nano-structured TiN thin films prepared by R, F. magnetron sputtering, Mater. Lett. 59 (2005) 3929–3932.
[8] A. Jafari, Z. Ghoranneviss, A.S. Elahi, M. Ghoranneviss, N.F. Yazdi, A. Rezaei, Effects of annealing on TiN thin film growth by DC magnetron sputtering, Adv. Mech. Eng. 6 (2014) 373847.
[9] G.V. Naik, B. Saha, J. Liu, S.M. Saber, E.A. Stach, J.M.K. Irudayaraj, T.D. Sands, M. Shalaev, A. Boltasseva, Epitaxial superlattices with titanium nitride as a plasmonic component for optical hyperbolic metamaterials, PNAS. 111 (2014) 7546–7551.
[10] S. Prayakarao, S. Robbins, N. Kinsey, A. Boltasseva, V.M. Shalaev, U.B. Wiesner, C. E. Bonner, R. Hussain, N. Noginova, M.A. Noginov, Gyroidal titanium nitride as nonmetallic metamaterial, Opt. Mater. Express, OME. 5 (2015) 1316–1322.
[11] Y. Krockenberger, S. Karimoto, H. Yamamoto, K. Semba, Coherent growth of superconducting TiN thin films by plasma enhanced molecular beam epitaxy, J. App. Phys. 112 (2012), 083920.
[12] W.-P. Guo, R. Mishra, C.-W. Cheng, B.-H. Wu, L.-J. Chen, M.-T. Lin, S. Gwo, Titanium nitride epitaxial films as a plasmonic material platform: alternative to gold, ACS Photonics. 6 (2019) 1848–1854.
[13] H.E. Rebenne, D.G. Bhat, Review of CVD TiN coatings for wear-resistant applications: deposition processes, properties and performance, Surf. Coat. Tech. 63 (1994) 1–13.
[14] R. Fix, R.G. Gordon, D.M. Hoffman, Chemical vapor deposition of titanium, zirconium, and hafnium nitride thin films, Chem. Mater. 3 (1991) 1138–1148.
[15] J. Su, R. Boichot, E. Blanquet, F. Mercier, M. Pons, Chemical vapor deposition of titanium nitride thin films: kinetics and experiments, Cryst. Eng. Comm. 21 (2019) 3974–3981.
[16] E. Langereis, S.B.S. Heil, M.C.M. van de Sanden, W.M.M. Kessels, In situ spectroscopic ellipsometry study on the growth of ultrathin TiN films by plasma-assisted atomic layer deposition, J. App. Phys. 100 (2006) 023534.
[17] J.A. Briggs, G.V. Naik, T.A. Petach, B.K. Baum, D. Goldhaber-Gordon, J.A. Dionne, Fully CMOS-compatible titanium nitride nanoantennas, Appl. Phys. Lett. 108 (2016), 051110.
[18] E. Shkondin, T. Repän, O. Takayama, A.V. Lavrinenko, High aspect ratio titanium nitride trench structures as plasmonic biosensor, Opt. Mater. Express, OME. 7 (2017) 4171–4182.
[19] I.-S. Yu, H.-E. Cheng, C.-C. Chang, Y.-W. Lin, H.-T. Chen, Y.-C. Wang, Z.-P. Yang, Substrate-insensitive atomic layer deposition of plasmonic titanium nitride films, Opt. Mater. Express, OME. 7 (2017) 777–784.
[20] S. Murai, K. Fujita, Y. Daido, R. Yasuhara, R. Kamakura, K. Tanaka, Plasmonic arrays of titanium nitride nanoparticles fabricated from epitaxial thin films, Opt. Express, OE. 24 (2016) 1143–1153.
[21] R.P. Sugavaneshwar, S. Ishii, T.D. Dao, A. Ohi, T. Nabatame, T. Nagao, Fabrication of highly metallic TiN films by pulsed laser deposition method for plasmonic applications, ACS Photonics. 5 (2018) 814–819.
[22] A. Torgovkin, S. Chaudhuri, A. Ruhtinas, M. Lahtinen, T. Sajavaara, I.J. Maasilta, High quality superconducting titanium nitride thin film growth using infrared pulsed laser deposition, Supercond. Sci. Technol. 31 (2018), 055017.
[23] L. Berthod, V. Gâté, M. Bichotte, M. Langlet, F. Vocanson, C. Jimenez, D. Jamon, I. Verrier, C. Veillas, O. Parriaux, Y. Jourlin, Direct fabrication of a metal-like TiN-based plasmonic grating using nitridation of a photo-patternable TiO_2 sol-gel film, Opt. Mater. Express, OME. 6 (2016) 2508–2520.
[24] A. Valour, M.A. Usuga Higuita, N. Crespo-Monteiro, S. Reynaud, M. Hochedel, D. Jamon, C. Donnet, Y. Jourlin, Micro-nanostructured TiN thin film: synthesis from a photo-patternable TiO_2 sol gel coating and rapid thermal nitridation, J. Phys. Chem. C 124 (2020) 25480–25488.
[25] O. Shavdina, L. Berthod, T. Kämpfe, S. Reynaud, C. Veillas, I. Verrier, M. Langlet, F. Vocanson, P. Fugier, Y. Jourlin, O. Dellea, Large area fabrication of periodic TiO_2 nanopillars using microsphere photolithography on a photopatternable sol–gel film, Langmuir. 31 (2015) 7877–7884.
[26] S. Briche, Z. Tebby, D. Riassetto, M. Messaoud, E. Gamet, E. Pernot, H. Roussel, O. Dellea, Y. Jourlin, M. Langlet, New insights in photo-patterned sol–gel-derived TiO_2 films, J. Mater. Sci. 46 (2011) 1474–1486.
[27] V. Gâté, Y. Jourlin, F. Vocanson, O. Dellea, G. Vercasson, S. Reynaud, D. Riassetto, M. Langlet, Sub-micrometric patterns written using a DIL method coupled to a TiO_2 photo-resist, Opt. Mater. 35 (2013) 1706–1713.

[28] G.E. Jellison, F.A. Modine, Parameterization of the optical functions of amorphous materials in the interband region, Appl. Phys. Lett. 69 (1996) 371–373.
[29] C.-C. Chang, J. Nogan, Z.-P. Yang, W.J.M. Kort-Kamp, W. Ross, T.S. Luk, D.A. R. Dalvit, A.K. Azad, H.-T. Chen, Highly plasmonic titanium nitride by room-temperature sputtering, Sci. Rep. 9 (2019) 1–9.
[30] J. Pflüger, J. Fink, W. Weber, K.P. Bohnen, G. Crecelius, Dielectric properties of TiC x , TiN x , VC x , and VN x from 1.5 to 40 eV determined by electron-energy-loss spectroscopy, Phys. Rev. B 30 (1984) 1155–1163.
[31] C.M. Zgrabik, E.L. Hu, Optimization of sputtered titanium nitride as a tunable metal for plasmonic applications, Opt. Mater. Express. 5 (2015) 2786.
[32] I. Senain, N. Nayan, H. Saim, Structural and electrical properties of TiO_2 thin film derived from sol-gel method using titanium (IV) butoxide, Int. J. Integr. Eng. 2 (2010) 8.
[33] P. Patsalas, N. Kalfagiannis, S. Kassavetis, G. Abadias, D.V. Bellas, Ch. Lekka, E. Lidorikis, Conductive nitrides: growth principles, optical and electronic properties, and their perspectives in photonics and plasmonics, Mater. Sci. Eng. R. Rep. 123 (2018) 1–55.
[34] H. Liang, J. Xu, D. Zhou, X. Sun, S. Chu, Y. Bai, Thickness dependent microstructural and electrical properties of TiN thin films prepared by DC reactive magnetron sputtering, Ceram. Int. 42 (2016) 2642–2647.
[35] D. Sosnin, D. Kudryashov, A. Mozharov, Investigation of electrical and optical properties of low temperature titanium nitride grown by rf-magnetron sputtering, J. Phys. : Conf. Ser. 917 (2017), 052025.
[36] L.J. Vandeperre, F. Giuliani, S.J. Lloyd, W.J. Clegg, The hardness of silicon and germanium, Acta Mater. 55 (2007) 6307–6315.
[37] X.Y. Zhou, Z.D. Jiang, H.R. Wang, Q. Zhu, A method to extract the intrinsic mechanical properties of soft metallic thin films based on nanoindentation continuous stiffness measurement technique, J. Phys.: Conf, Ser. 48 (2006) 1096–1101.
[38] W.C. Oliver, G.M. Pharr, An improved technique for determining hardness and elastic- modulus using load and displacement sensing indentation experiments, J. Mater. Res. 7 (1992) 1564–1583.
[39] J.L. Loubet, M. Bauer, A. Tonck, S. Bec, B. Gauthier-Manuel, Nano-indentation with a surface force apparatus, NATO Adv. Study Inst. Ser. E. (1993) 429–447.
[40] R. Saha, W.D. Nix, Effects of the substrate on the determination of thin film mechanical properties by nanoindentation, Acta Mater. 50 (2002) 23–38.
[41] Handbook of Refractory Carbides and Nitrides - 1st Edition, (1996).